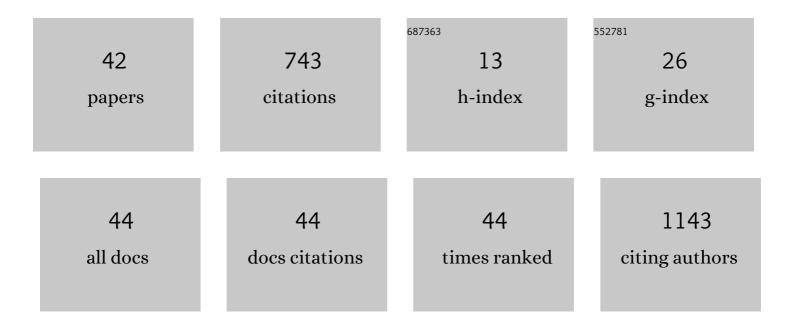
## Amol S Pednekar

List of Publications by Year in descending order

Source: https://exaly.com/author-pdf/5117763/publications.pdf Version: 2024-02-01



#	Article	IF	CITATIONS
1	Performance of Câ€5ENSE Accelerated Rapid Liver Shear Stiffness Measurement Using Displacement Wave Polarityâ€Inversion Motion Encoding: An Evaluation Study. Journal of Magnetic Resonance Imaging, 2022, , .	3.4	2
2	Myocardial Parametric Mapping by Cardiac Magnetic Resonance Imaging in Pediatric Cardiology and Congenital Heart Disease. Circulation: Cardiovascular Imaging, 2022, 15, CIRCIMAGING120012242.	2.6	9
3	Fusing acceleration and saturation techniques with wave amplitude labeling of timeâ€shifted zeniths MR elastography. Magnetic Resonance in Medicine, 2021, 85, 1552-1560.	3.0	1
4	Assessment of agreement between manual and automated processing of liver MR elastography for shear stiffness estimation in children and young adults with autoimmune liver disease. Abdominal Radiology, 2021, 46, 3927-3934.	2.1	5
5	Comparison of compressed SENSE and SENSE for quantitative liver MRI in children and young adults. Abdominal Radiology, 2021, 46, 4567-4575.	2.1	7
6	Agreement Between Automated and Clinically-Reported Manual ROIBased MR Elastography Liver Stiffness Measurements in Children and Young Adults. American Journal of Roentgenology, 2021, , 1-2.	2.2	2
7	Dobutamine stress cardiac MRI is safe and feasible in pediatric patients with anomalous aortic origin of a coronary artery (AAOCA). International Journal of Cardiology, 2021, 334, 42-48.	1.7	29
8	Ultrafast Computation of Left Ventricular Ejection Fraction by Using Temporal Intensity Variation in Cine Cardiac Magnetic Resonance. Texas Heart Institute Journal, 2021, 48, .	0.3	0
9	Quantitative assessment of velocity and flow using compressed SENSE in children and young adults with adequate acquired temporal resolution. Journal of Cardiovascular Magnetic Resonance, 2021, 23, 113.	3.3	8
10	Breath-hold and free-breathing quantitative assessment of biventricular volume and function using compressed SENSE: a clinical validation in children and young adults. Journal of Cardiovascular Magnetic Resonance, 2020, 22, 54.	3.3	35
11	Mitral Valve Flow and Myocardial Motion Assessed with Dual-Echo Dual-Velocity Cardiac MRI. Radiology: Cardiothoracic Imaging, 2020, 2, e190126.	2.5	2
12	Newly Developed Methods for Reducing Motion Artifacts in Pediatric Abdominal MRI: Tips and Pearls. American Journal of Roentgenology, 2020, 214, 1042-1053.	2.2	30
13	Regadenoson Stress Perfusion Cardiac Magnetic Resonance Imaging in Children With Kawasaki Disease and Coronary Artery Disease. American Journal of Cardiology, 2019, 124, 1125-1132.	1.6	20
14	Free-breathing Cardiorespiratory Synchronized Cine MRI for Assessment of Left and Right Ventricular Volume and Function in Sedated Children and Adolescents with Impaired Breath-holding Capacity. Radiology: Cardiothoracic Imaging, 2019, 1, e180027.	2.5	5
15	Myocardial Stress Perfusion MRI Using Regadenoson: A Weight-based Approach in Infants and Young Children. Radiology: Cardiothoracic Imaging, 2019, 1, e190061.	2.5	10
16	High frame rate cardiac cine MRI for the evaluation of diastolic function and its direct correlation with echocardiography. Journal of Magnetic Resonance Imaging, 2019, 50, 1571-1582.	3.4	6
17	Interleaved susceptibilityâ€weighted and FLAIR MRI for imaging lesionâ€penetrating veins in multiple sclerosis. Magnetic Resonance in Medicine, 2018, 80, 1132-1137.	3.0	6
18	Platform for Automated Real-Time High Performance Analytics on Medical Image Data. IEEE Journal of Biomedical and Health Informatics, 2018, 22, 318-324.	6.3	1

Amol S Pednekar

#	Article	IF	CITATIONS
19	Two-center clinical validation and quantitative assessment of respiratory triggered retrospectively cardiac gated balanced-SSFP cine cardiovascular magnetic resonance imaging in adults. Journal of Cardiovascular Magnetic Resonance, 2018, 20, 44.	3.3	17
20	Patientâ€specific 3D FLAIR for enhanced visualization of brain white matter lesions in multiple sclerosis. Journal of Magnetic Resonance Imaging, 2017, 46, 557-564.	3.4	2
21	GRAPE: a graphical pipeline environment for image analysis in adaptive magnetic resonance imaging. International Journal of Computer Assisted Radiology and Surgery, 2017, 12, 449-457.	2.8	1
22	Automated patientâ€specific optimization of threeâ€dimensional doubleâ€inversion recovery magnetic resonance imaging. Magnetic Resonance in Medicine, 2016, 75, 585-593.	3.0	10
23	Shortâ€Term Repeatability of Magnetic Resonance Elastography at 3.0T: Effects of Motionâ€Encoding Gradient Direction, Slice Position, and Meal Ingestion. Journal of Magnetic Resonance Imaging, 2016, 43, 704-712.	3.4	10
24	Comparison of two single-breath-held 3-D acquisitions with multi-breath-held 2-D cine steady-state free precession MRI acquisition in children with single ventricles. Pediatric Radiology, 2016, 46, 637-645.	2.0	7
25	Ultrafast computation of left ventricular ejection fraction using temporal intensity variation in cine steady-state free precession cardiac MR images with or without contrast. Journal of Cardiovascular Magnetic Resonance, 2016, 18, 085.	3.3	Ο
26	Effect of respiratory suspension on the computation of volume-based early peak filling rate to late peak filling rate ratio. Journal of Cardiovascular Magnetic Resonance, 2016, 18, O93.	3.3	0
27	A framework for precision magnetic resonance imaging: Initial results. , 2016, , .		3
28	Clinical validation of free breathing respiratory triggered retrospectively cardiac gated cine balanced steady-state free precession cardiovascular magnetic resonance in sedated children. Journal of Cardiovascular Magnetic Resonance, 2015, 17, 1.	3.3	111
29	Pancreatic adenocarcinoma: a pilot study of quantitative perfusion and diffusion-weighted breath-hold magnetic resonance imaging. Abdominal Imaging, 2014, 39, 744-752.	2.0	20
30	Clinical validation of free breathing Respiratory Triggered Retrospectively Cardiac Gated Cine Steady-State Free Precession (RT-SSFP) imaging in sedated children. Journal of Cardiovascular Magnetic Resonance, 2013, 15, .	3.3	2
31	Evaluation of a Subject specific dual-transmit approach for improving B1 field homogeneity in cardiovascular magnetic resonance at 3T. Journal of Cardiovascular Magnetic Resonance, 2013, 15, 68.	3.3	29
32	Functional Morphology Analysis of the Left Anterior Descending Coronary Artery in EBCT Images. IEEE Transactions on Biomedical Engineering, 2010, 57, 1886-1896.	4.2	2
33	High temporal resolution SSFP cine MRI for estimation of left ventricular diastolic parameters. Journal of Magnetic Resonance Imaging, 2010, 31, 872-880.	3.4	27
34	Feasibility and validation of estimating Global LV functional indices from limited projections using a Modified Simpson's Algorithm. Journal of Cardiovascular Magnetic Resonance, 2010, 12, .	3.3	0
35	Ultrafast in-line computation of ejection fraction from cardiac cine steady-state free precession (SSFP) images. Journal of Cardiovascular Magnetic Resonance, 2010, 12, .	3.3	0
36	Localization and Segmentation of Left Ventricle in Cardiac Cine-MR Images. IEEE Transactions on Biomedical Engineering, 2009, 56, 1360-1370.	4.2	65

Amol S Pednekar

#	Article	IF	CITATIONS
37	Determining exerciseâ€induced blood flow reserve in lower extremities using phase contrast MRI. Journal of Magnetic Resonance Imaging, 2008, 27, 1096-1102.	3.4	8
38	Automatic computation of left ventricular ejection fraction from spatiotemporal information in cine‣SFP cardiac MR images. Journal of Magnetic Resonance Imaging, 2008, 28, 39-50.	3.4	13
39	Image segmentation based on fuzzy connectedness using dynamic weights. IEEE Transactions on Image Processing, 2006, 15, 1555-1562.	9.8	59
40	Automated Left Ventricular Segmentation in Cardiac MRI. IEEE Transactions on Biomedical Engineering, 2006, 53, 1425-1428.	4.2	132
41	Automatic identification of the left ventricle in cardiac cine-MR images: Dual-contrast cluster analysis and scout-geometry approaches. Journal of Magnetic Resonance Imaging, 2006, 23, 641-651.	3.4	23
42	Automatic Segmentation of Abdominal Fat from CT Data. , 2005, , .		22